Research Square

Preprints are preliminary reports that have not undergone peer review.
They should not be considered conclusive, used to inform clinical practice,
or referenced by the media as validated information.

# Targeted gene panel versus whole-exome sequencing for prenatally diagnosed Human laterality defects

**Yuan Chen**
Women's Hospital, School of Medicine, Zhejiang University
**Yeqing Qian**
Women's Hospital, School of Medicine, Zhejiang University
**Pengfei Xu**
Zhejiang University School of Medicine
**Qiong Luo**
luoq@zju.edu.cn

Women's Hospital, School of Medicine, Zhejiang University

**Research Article**

**Keywords:** laterality defects, targeted gene panel, whole-exome sequencing, prenatal diagnosis

**Posted Date:** June 19th, 2026

**DOI:** https://doi.org/10.21203/rs.3.rs-9941419/v1

**License:** This work is licensed under a Creative Commons Attribution 4.0 International License. Read Full License

**Additional Declarations:** No competing interests reported.

## Abstract

# Background

Laterality defects, congenital disorders characterized by abnormal left-right asymmetry, are increasingly diagnosed prenatally due to advances in imaging. However, their etiology remains complex, with only 15–20% linked to genetic anomalies. This study developed a targeted gene panel for laterality defects and compared its diagnostic performance with whole-exome sequencing (WES) in prenatal settings.

# Results

A custom panel encompassing 98 genes (46 OMIM-associated, 52 implicated in animal models of laterality development) was designed. 19 prenatal cases with *situs inversus* or heterotaxy syndrome (HTX) were analyzed using both the panel and WES. Metrics including coverage, sequencing depth (200×/300× thresholds), detection rates, and variant discrepancies were compared. The panel achieved a 94.7% detection rate, identifying 3 novel candidate genes (*MYO1D, DNAH6, RFX3*). In WES-tested cases (n = 16), the detection rate was 75.0%, with 10 variants undetected by the panel. The panel demonstrated superior average read depth and significantly higher coverage of clinically critical genomic regions across thresholds compared to WES.

# Conclusions

The targeted panel demonstrated superior diagnostic yield, data quality, and cost-effectiveness compared to WES, establishing its utility as a robust screening tool for prenatally diagnosed laterality defects. Its clinical applicability is further strengthened by shorter turnaround times and precise interrogation of disease-associated loci, positioning it as a pragmatic alternative to WES for prenatal genetic evaluation and discovery of novel pathogenic variants underlying laterality anomalies.

## 1. Introduction

Laterality defects are characterized by an atypical disposition of the thoracoabdominal organs as well as blood vessels along the left-right axis, including *situs inversus* (complete or partial reversal of normal chest and abdominal organs position) and heterotaxy (any other abnormalities of left-right development). Although s*itus inversus* usually exhibit benign clinical courses, HTX is commonly associated with numerous intricate cardiac abnormalities and tends to have a rather poor prognosis [1, 2].

The estimated prevalence of laterality defects is around 1 in 15,000 individuals. HTX has an incidence of approximately 1 per 10,000 live births, while *situs inversus* demonstrates a broader epidemiological range, with reported incidence rates spanning from 1 in 6,500 to 1 in 25,000 live births [2, 3]. As reported, approximately 50% of primary ciliary dyskinesia (PCD) patients present with laterality defects (also named Kartagener syndrome), of which 41.0% are *situs inversus* and 12.1% are HTX [4]. Since the underlying etiology of PCD involves structural and functional defects in airway cilia, the predominant clinical manifestations characteristically include recurrent infections affecting both the upper and lower respiratory tracts. The implementation of genetic testing for early diagnosis of PCD is essential to mitigate disease progression and clinical severity in chronic pulmonary disorders, while concurrently enabling prognostic stratification and optimization of patient quality of life [5].

The etiologies of laterality defects are complicated, involving environmental and genetic factors. Besides the poorly identified environmental factors, the known genetics causes have been reported to account for over 15%-20% [6, 7]. As previously reported, chromosomal abnormalities are rare (3%–4%) in laterality defects [8, 9]. Thus the application of expanded gene panels or or WES enables targeted identification of monogenic etiologies, despite the precise molecular pathways and genetic determinants underlying laterality defects remain incompletely characterized. Notably, a significant proportion of genetic loci implicated in left-right axis patterning within model organisms remain to be comprehensively investigated for their potential involvement in human congenital laterality disorders [2, 3].

According to contemporary scientific consensus, prenatal phenotyping combined with advanced genomic technologies, especially next-generation sequencing (NGS), augments diagnostic precision in identifying pathogenic genetic variants during the prenatal period. WES has been widely used in the prenatal diagnosis of structurally abnormal fetuses. However, WES has limitations in breadth and depth of coverage for some specific disease-causing genes, large and complex data managing. Targeted gene panel sequencing offers an alternative to minimize possible false negatives [10].

From this consideration, we designed a targeted gene panel with 98 genes specifically related to laterality defects. Our study aimed to compare the diagnostic efficacy of targeted panel sequencing and WES for prenatal diagnosed isolated s*itus inversus* and HTX, after confirming negative results by conventional karyotypes and chromosomal microarray analysis (CMA).

## 2. Materials and Methods

# 2.1 Participants

A retrospective cohort analysis was conducted on prenatally diagnosed cases of *situs inversus* or HTX identified through ultrasonographic screening and fetal echocardiography at Women's Hospital, Zhejiang University, School of Medicine (Hangzhou, China) between April 2016 and October 2022. Fetal biological specimens, including amniotic fluid and umbilical cord blood via invasive prenatal diagnostic procedure were collected at varying gestational ages. Post-termination fetal muscle specimens were obtained through surgical dissection following elective pregnancy termination procedures, and postnatal

peripheral blood was collected for live birth as an alternative in one case. Comprehensive perinatal information including gestational age at initial diagnosis, relevant familial history, detailed prenatal imaging records and obstetric outcomes were systematically abstracted from electronic medical records.

## 2.2 Construction of the targeted gene panel

The targeted gene panel was developed using Agilent's SureDesign platform, incorporating 98 disease-associated genes. 46 known genes are curated from OMIM database (https://www.omim.org) related to *situs inversus* or heterotaxy, and the other 52 genes are selected based on reported experimental evidence of their role in zebrafish left-right axis patterning. The complete gene list and information is detailed in Supplementary Table 1.

## 2.3 DNA extraction and sequencing

Fetal genomic DNA was extracted from various fetal samples, including amniotic fluid, cord blood and fetal tissues, using the MagPure Universal DNA Kit (Magen Biotech) according to the manufacturer's procedures. Within the cohort, peripheral blood was obtained from one patient after birth. gDNA were sheared to 150–200 bp target DNA fragments. The DNA library was constructed using a TargetSeq One® Hyb & Wash Kit (iGene Tech), while high-throughput sequencing was performed on an Illumina NovaSeq 6000 platform with PE150.

## 2.4 WES Analysis

WES was performed at the Shenzhen Huada Medical Laboratory (BGI) using standardized protocols. Genomic DNA encompassing the target gene exons and adjacent splice regions was subjected to capture and enrichment using the Roche KAPA HyperExome kits. Subsequent mutation screening was performed via next-generation sequencing platforms (MGISEQ-2000 or DNBSEQ-T7) with standardized quality control metrics. The sequencing data met stringent quality criteria, demonstrating a mean read depth ≥ 200× across the target regions, with > 98.5% of genomic positions achieving coverage exceeding 20× depth threshold.

## 2.5 Variant detection and filtering

After sequencing, raw FASTQ data were obtained and processed through the following steps: a) map the short reads to a reference genome (hg19) using the BWA software (sentieon) [11] to determine the position of the short sequences on the genome; b) use the SAMtools software (v1.9) to sort the short sequences and convert the format of the data; c) use the Picard software (v1.134) (http://broadinstitute.github.io/picard/) to mark duplicate reads; d) use the Genome Analysis Toolkit (sentieon)[12] to find sites with differences (including SNVs and indels) between sample sequence data and the reference genome; and e) perform functional annotation of these variant sites using the VEP software (104.3). The gnomAD v2.1.1, Exome Aggregation Consortium (0.3.1), 1000 Genomes Project, ESP6500, ClinVar and other public databases were used to screen the variants.

## 2.6 Classification of all reported variants

A systematic search of OMIM database and published literature was conducted to identify candidate genes implicated in human left-right axis determination. Custom-designed probes targeting the exonic regions of these genes were subsequently employed for genomic capture. All identified variants underwent pathogenicity classification according to the American College of Medical Genetics and Genomics (ACMG) guidelines for sequence variant interpretation [13]. Variants were categorized into three distinct groups: (1) pathogenic/likely pathogenic variants in established disease genes associated with visceral laterality defects; (2) variants of uncertain significance (VUS) in genes with known postnatal disease associations but undocumented roles in embryonic development; (3) Novel variants in genes not previously associated with human developmental disorders, proposed here as potential contributors to visceral situs anomalies based on functional and segregation evidence.

## 2.7 Sanger sequencing confirmation

All genetic variants identified as potentially diagnostic were confirmed through sanger sequencing.

## 2.8 Coverage analysis of WES and targeted amplicon panel

Each sample from the WES and panel assays underwent initial processing with Trim Galore (https://github.com/FelixKrueger/TrimGalore) to remove adapter sequences and low-quality bases. The trimmed reads were mapped to the GRCh38 reference genome using BWA-MEM (https://arxiv.org/abs/1303.3997). Alignments were then sorted, and duplicates were marked using Samtools (https://doi.org/10.1093/bioinformatics/btp352). To focus on the targeted genomic regions, Bedtools Intersect (https://doi.org/10.1093/bioinformatics/btq033) was used to retain genome positions covered by the panel probe regions for downstream analysis. The average genome coverage of the targeted bases within the panel probe regions was calculated with Samtools, and read counts from panel assay samples were down-sampled to match the read counts of their corresponding WES samples using Samtools. Finally, the mean coverage for each sample, along with depth at various specified coverage thresholds, was quantified using Qualimap2 [14], with coverage calculations restricted to regions defined by the panel capture design.

# 3. Results

## 3.1 Patient characteristics

Following exclusion of cases with chromosomal karyotypic abnormalities and pathogenic copy number variations (CNVs), this cohort comprised 19 prenatally diagnosed cases of laterality defects (median gestational age at diagnosis: 25 weeks; range: 14–32 weeks) undergoing targeted gene panel sequencing and WES. Detailed phenotypic characteristics, including cardiovascular/extra-cardiac anomalies and pregnancy outcomes, are summarized in Table 1.

Table 1
Demographic and clinical data of 19 probands with laterality defects included in the study

| Case No. | Gestational Age(GA) | Gender | Laterality defects | Associated congenital heart defects | Other non-cardiac structural anomalies | Pregnancy Outcome |
|---|---|---|---|---|---|---|
| 1 | 25 | female | *situs inversus* | dextrocardia | - | live birth |
| 2 | 16 | male | HTX | mitral atresia, left ventricular hypoplasia, double-outlet right ventricle, pulmonary artery hypoplasia, partial endocardial cushion defect | - | elective abortion |
| 3 | 26 | male | HTX | levocardia, complete endocardial cushion defect; double-outlet right ventricle; right aortic arch; the diameter of the pulmonary artery is narrow and the flow velocity is fast | - | elective abortion |
| 4 | 27 | male | HTX | interrupted inferior vena cava with dilatation of the azygos vein | - | live birth |
| 5 | 28 | male | *situs inversus* | dextrocardia | - | elective abortion |
| 6 | 25 | male | *situs inversus* | ventricular septal defect | - | live birth |
| 7 | 32 | male | *situs inversus* | dextrocardia | - | elective abortion |

The cohort included 9 cases (47.4%) of *situs inversus* and 10 cases (52.6%) of HTX, with 12 cases demonstrating cardiovascular anomalies (8 complex congenital heart defects) and 1 case exhibiting an extra-cardiac malformation (right pelvic ectopic kidney). Fetal sex distribution was 12 males and 7 females, with 8 elective terminations and 11 live births. All probands had non-consanguineous parents without family histories of visceral situs anomalies or PCD. Notably, two maternal histories revealed adverse reproductive outcomes: one previous child with glucose-6-phosphate dehydrogenase deficiency and one prior pregnancy terminated at 13 weeks due to fetal hydrocephalus.

## 3.2 Coverage analysis of targeted gene panel sequencing and WES

To enable a fair and meaningful comparison between WES and targeted gene panel sequencing, the read depth of samples sequenced with the targeted panel was downsampled to match the corresponding read depth observed in WES for the shared target regions. Both WES and targeted gene panel sequencing consistently achieved high coverage, with ≥ 100× read depth across most targeted genomic positions. However, targeted gene panel sequencing yielded higher average read coverage within the target space across all samples, particularly at more stringent thresholds of 200× and 300× (Fig. 1A and 1B). Across varying sample-level coverage thresholds, targeted gene panel sequencing consistently outperformed WES in the number of genomic positions reaching the specified thresholds, highlighting its enhanced capacity for deep and reliable coverage in clinically relevant regions (Fig. 2).

## 3.3 Identified variants using targeted gene panel vs. WES

Following variant filtering, we identified 60 variants across 11 genes in 18 out of 19 patients in our cohort using a customized gene panel (Table 2), achieving a total diagnostic rate of 94.7%. Among these, the *DNAH5* gene was the most frequently affected, with variants identified in 9 out of 19 patients, followed by *DNAH11* (7/19), *DNAH9* (3/19), *DNAH6* (2/19), and single occurrences in *ZIC3*, *MYO1D*, *ACVR2B*, *DNAAF3*, *PKD1L1*, *RFX3* and *FOXJ1* (1/19 each). WES was systematically performed on 16 biological specimens under standardized experimental conditions. Case 10, 15, 17 were excluded from WES analysis due to insufficient sample volume. Using WES alone, no variation was detected in case 6,7, 11 and 12 of the 16 patients, with an overall diagnostic rate of 75.0%. WES corroborated the panel results by identifying 16 consistent variants. WES detected 10 additional variants that were not identified by the panel, including *MMP21*, *BBS*, *DNAH9, DNAH11, CFAP53* and *HYDIN* gene. Additionally, *MYO1D*, *DNAH6*, and *RFX3*, which were not associated with human diseases in OMIM database right now, were identified only using the targeted gene panel in patients 3, 6, 10 and 17, respectively. Based on the targeted panel and WES sequencing results, 68 variants included 7 LP variants and 61 VUS variants according to ACMG criteria. The majority of diagnoses (12/15, 80.0%) were autosomal recessive, while *ACVR2B, FOXJ1* were autosomal dominant and *ZIC3* was X-linked recessive.

Table 2
Detected variants of 19 patients by targeted gene panel and WES.

| Patient no. | Targed gene panel | | | | | | | | Pane WES |
|---|---|---|---|---|---|---|---|---|---|
| | Gene (OMIM) | Accession No. | Inheritance Mode | Location | Variants | Amino acids change | Gene Type | ACMG Classification | Cons or N |
| 1 | *DNAH9* (618300) | NM_001372.4 | AR | Ex1/69 | c.308del | p.F103Sfs*31 | het | LP (PSV1+PM2_Supporting) | Yes |
| | | | | In25/68 | c.5391 + 78G > A | / | het | VUS (PM2_Supporting) | No, V |
| | | | | In45/68 | c.8707 + 80G > C | / | het | VUS (PM2_Supporting) | No, V |
| 2 | *ZIC3* (306955) | NM_003413.4 | XLR | Ex3/3 | c.1391A > C | p.E464A | hemi | VUS (PM2_Supporting) | Yes |
| 3 | *DNAH11* (611884) | NM_001277115.2 | AR | Ex81/82 | c.13165_13168dup | p.M4390Nfs*10 | het | LP (PVS1+PM2_Supporting) | Yes |
| | | | | Ex14/82 | c.2619dup | p.Y874Ifs*19 | het | LP PVS1+PM2_Supporting) | Yes |
| | | | | Ex9/82 | c.1649G > A | p.R550L | het | VUS (PM2_Supporting) | No, V |
| | *DNAH9* (618300) | NM_001372.4 | AR | Ex20/69 | c.4441A > G | p.N1481D | het | VUS (PM2_Supporting) | No, V |
| | | | | In62/68 | c.11878-185G > A | | het | VUS (PM2_Supporting) | No, V |
| | *MYO1D*# | NM_015194.3 | - | Ex18/22 | c.2419G > A | p.V807M | het | VUS (PM2_Supporting) | No, V |
| | | | | In5/21 | c.619-182G > A | | het | VUS (PM2_Supporting) | No, V |
| 4 | *DNAH11* (611884) | NM_001277115.2 | AR | Ex18/82 | c.3470T > G | p.L1157R | het | VUS (PM2_Supporting+ PM3_Strong+PP3) | Yes |
| | | | | Ex78/82 | c.12890G > A | p.R4297Q | het | VUS (PM2_Supporting +BP4) | Yes |
| 5 | *DNAH5* (608644) | NM_001369.3 | AR | In46/78 | c.7752 + 3A > G | / | het | VUS (PM2_Supporting +PP3) | Yes |
| | | | | Ex5/79 | c.451A > G | p.N151D | het | VUS (PM2_Supporting+BP1) | Yes |
| 6 | *DNAH5* (608644) | NM_001369.3 | AR | Ex31/79 | c.5002C > T | p.R1668W | het | VUS (PM2_Supporting +PP3) | No, V |
| | | | | Ex72/79 | c.12367C > T | p.H4123Y | het | VUS (PM3 + BS1) | No, V |
| | *DNAH6*# | NM_001370.2 | - | Ex11/77 | c.1673C > T | p.S558L | het | VUS (PM2_Supporting+BP4) | No, V |
| | | | | Ex57/77 | c.9439G > A | p.G3147S | het | VUS (PM2_Supporting) | No, V |
| 7 | *ACVR2B* (613751) | NM_001106.4 | AD | Ex11/11 | c.*172A > G | / | het | VUS (PM2_Supporting) | No, V |
| 8 | Negative | | | | | | | | No, V (+), M |
| 9 | *DNAAF3* (606763) | NM_001256714.1 | AR | Ex7/12 | c.868-3_871dup | p.Q291Pfs*21 | het | LP (PVS1+PM2_Supporting) | Yes |

ACMG, American College of Medical Genetics and Genomics

het, heterozygous variant

hemi, hemizygous variant

P, pathogenic;

LP, likely pathogenic;

VUS, variant of unknown significance

AR, autosomal recessive;

AD, autosomal dominant

XLR, X-linked recessive

#, superscript indicates that the inheritance pattern is unclear

| Patient no. | Targed gene panel | | | | | | | | Pane WES |
|---|---|---|---|---|---|---|---|---|---|
| | Gene (OMIM) | Accession No. | Inheritance Mode | Location | Variants | Amino acids change | Gene Type | ACMG Classification | Cons or N |
| | | | | Ex10/12 | c.1336C > T | p.R446* | het | LP (PVS1+PM2_Supporting) | Yes |
| | | | | Ex9/12 | c.1235C > G | p.Pro412R | het | VUS (PM2_Supporting) | Yes |
| | *DNAH11* (611884) | NM_001277115.2 | AR | In18/81 | c.3648 + 4A > G | / | het | VUS (PM2_Supporting) | No, V |
| | | | | In46/81 | c.7645 + 83C > A | / | het | VUS (PM2_Supporting) | No, V |
| | | | | In81/81 | c.13303 + 177C > A | / | het | VUS (PM2_Supporting) | No, V |
| **10** | *DNAH6*# | NM_001370.2 | - | Ex30/77 | c.4615C > G | p.Q1539E | het | VUS (PM2_Supporting) | Unav |
| | | | | Ex30/77 | c.4615C > G | p.Q1539E | het | VUS (PM2_Supporting) | |
| **11** | *DNAH11* (611884) | NM_001277115.2 | AR | Ex76/82 | c.12428T > C | p.M4143T | het | VUS (PM2_Supporting) | No, V |
| | | | | In60/81 | c.9925-91A > C | | het | VUS (PM2_Supporting) | No, V |
| | *DNAH5* (608644) | NM_001369.3 | AR | In38/78 | c.6445-213T > C | | het | VUS (PM2_Supporting) | No, V |
| | | | | In29/78 | c.4797-143T > C | | het | VUS (PM2_Supporting) | No, V |
| **12** | *DNAH5* (608644) | NM_001369.3 | AR | In7/78 | c.975 + 6C > T | | het | VUS (PM2_Supporting) | No, V |
| | | | | In25/78 | c.4053 + 76T > C | | het | VUS (PM2_Supporting) | No, V |
| **13** | *DNAH5* (608644) | NM_001369.3 | AR | Ex24/79 | c.3613G > A | p.A1205T | het | VUS (PM2_Supporting) | No, V dete *BBS*: c.15 G an c.94 |
| | | | | In 18/78 | c.2744-169T > C | | het | VUS (PM2_Supporting) | |
| | | | | In7/19 | c.1160-98C > T | | het | VUS (PM2_Supporting) | |
| | *DNAH11* (611884) | NM_001277115.2 | AR | Ex69/82 | c.11352C > A | p.F3784L | het | VUS (PM2_Supporting) | |
| | | | | In52/81 | c.8674-74C > G | | het | VUS (PM2_Supporting) | |
| **14** | *DNAH5* (608644) | NM_001369.3 | AR | Ex67/79 | c.11506G > A | p.V3836I | het | VUS (PM2_Supporting) | Yes |
| | | | | In28/78 | c.4596 + 5A > C | | het | VUS (BS1) | Yes |
| | Negative | | | | | | | | No, V dete *DNA* c.92 c.18 G |
| **15** | *DNAH5* (608644) | NM_001369.3 | AR | In36/78 | c.6061 + 145G > A | | het | VUS (PM2_Supporting) | No, V |
| | | | | Ex36/79 | c.5966C > A | p.T1989N | het | VUS (PM2_Supporting) | |
| | | | | In65/78 | c.11211 + 62A > G | | het | VUS (PM2_Supporting) | |
| | | | | In48/78 | c.8011-55A > C | | het | VUS (PM2_Supporting) | |
| **16** | *DNAH11* (611884) | NM_001277115.2 | AR | In23/81 | c.4254 + 44A > G | | het | VUS (PM2_Supporting) | No, V dete *DNA* c.88 T |
| | | | | In24/81 | c.4378-102G > C | | het | VUS (PM2_Supporting) | |

ACMG, American College of Medical Genetics and Genomics

het, heterozygous variant

hemi, hemizygous variant

P, pathogenic;

LP, likely pathogenic;

VUS, variant of unknown significance

AR, autosomal recessive;

AD, autosomal dominant

XLR, X-linked recessive

#, superscript indicates that the inheritance pattern is unclear

| Patient no. | Targed gene panel | | | | | | | | Pane WES |
|---|---|---|---|---|---|---|---|---|---|
| | Gene (OMIM) | Accession No. | Inheritance Mode | Location | Variants | Amino acids change | Gene Type | ACMG Classification | Cons or N |
| | | | | In27/81 | c.4818-43T > C | | het | VUS (PM2_Supporting) | |
| 17 | *DNAH9* (618300) | NM_001372.4 | AR | In22/68 | c.4873-263T > G | | het | VUS (PM2_Supporting) | Unav |
| | | | | In39/68 | c.7718 + 300C > T | | het | VUS (PM2_Supporting) | |
| | *PKD1L1* (617205) | NM_138295.5 | AR | In47/56 | c.7090-208C > T | | het | VUS (PM2_Supporting) | |
| | | | | In32/56 | c.5153 + 67C > T | | het | VUS (PM2_Supporting) | |
| | *RFX3*[#] | NM_134428.3 | - | In13/17 | c.1455 + 51A > G | | het | VUS (PM2_Supporting) | |
| 18 | *DNAH11* (611884) | NM_001277115.2 | AR | Ex24/82 | c.4306C > T: | p.R1436W | het | VUS (BS1) | No, V |
| | | | | Ex76/82 | c.12407G > A: | p.R4136H | het | VUS (PM2_Supporting +PP3) | Yes |
| | *DNAH5* (608644) | NM_001369.3 | AR | Ex68/79 | c.11664C > G: | p.Y3888* | het | LP (PVS1+PM2_Supporting) | Yes |
| 19 | *FOXJ1* (618699) | NM_001454.4 | AD | Ex3/3 | c.551G > A | p.R184Q | het | VUS (PM2_Supporting +PP3) | Yes |
| | *DNAH5* (608644) | NM_001369.3 | AR | In63/78 | c.10873-213A > G | | het | VUS (PM2_Supporting) | No, V |
| | | | | In59/78 | c.10102-193A > C | | het | VUS (PM2_Supporting) | |
| | | | | In5/78 | c.661-173C > T | | het | VUS (PM2_Supporting) | |

ACMG, American College of Medical Genetics and Genomics

het, heterozygous variant

hemi, hemizygous variant

P, pathogenic;

LP, likely pathogenic;

VUS, variant of unknown significance

AR, autosomal recessive;

AD, autosomal dominant

XLR, X-linked recessive

#, superscript indicates that the inheritance pattern is unclear

## 4. Discussion

In this investigation, we conducted targeted sequencing using a custom-designed gene panel encompassing 98 candidate loci in 19 cases of prenatally diagnosed HTX and *situs inversus*. For 16 subjects within this cohort, a comparative analysis was performed between the panel sequencing outcomes and corresponding WES data, focusing on coverage efficiency and variant detection accuracy. To our knowledge, this work represents the first systematic comparative evaluation of targeted panel sequencing versus WES within a prenatal diagnostic cohort. Furthermore, our panel design innovatively integrates 46 OMIM-classified laterality defects-associated pathogenic genes and 52 additional loci that, while not yet definitively associated with human HTX or *situs inversus* in OMIM entries, have demonstrated functional relevance to left-right axis patterning in experimental animal models. This expanded methodology effectively compensates for the limited diagnostic yield of targeted gene panels, which predominantly rely on previously documented gene sequencing data, thereby significantly improving variant detection rates.

## Technical Performance Comparison

Targeted panel sequencing demonstrated superior technical performance compared to WES in our study. The higher average raw sequencing depth of the panel (368x vs. 296x for WES) enabled more reliable detection of low-frequency variants. More importantly, downsampling analysis of panel data to match WES coverage showed that, at equivalent coverage levels, the panel provided superior genome coverage across various sequencing depth thresholds. This suggests that the targeted approach offers more reliable detection of regions of interest compared to WES.

The targeted gene panel identified LP/VUS variants in 94.7% of cases, surpassing WES (75.0%), primarily due to improved resolution of variants in *MYO1D*, *DNAH6*, and *RFX3*, genes only validated to be critical for left-right patterning in model organisms based on the researches so far and the increased intron detection rate. 29 WES-missed variants (Table 2) were detected by the panel, highlighting its enhanced sensitivity for known disease-associated loci.

The per-sample cost of targeted sequencing (1,000RMB) was markedly lower than WES (4,800RMB). The panel's focused design reduced bioinformatics burdens, cutting data storage costs by 79% compared to WES. For clinics prioritizing cost containment, panels offer a sustainable first-tier option, particularly in resource-limited settings.

The panel reduced turnaround time by 7 days (7 vs.25 days for WES), critical for time-sensitive prenatal decisions. This acceleration stems from streamlined analysis of 98 candidate genes versus WES's exome-wide burden. Rapid reporting complies with ACMG guidelines recommending a faster turnaround for prenatal genetic testing [15]. This accelerated process enables informed decision-making regarding pregnancy continuation, obstetric management, delivery planning, and neonatal care interventions, when clinically applicable.

## Positive variants

In our cohort, *DNAH5* mutations accounted for the majority of identified variants, aligning with previous studies that highlight its recurrent involvement in PCD [5, 16, 17]. The *DNAH5* gene produces dynein axonemal heavy chain 5, critical for ciliary motility and structural stability. This molecular motor mediates coordinated ciliary beating required for mucociliary clearance. *DNAH5* mutations disrupting dynein arm assembly impair motility (50%), causing Kartagener syndrome manifestations: *situs inversus*, chronic sinusitis, and bronchiectasis [5]. Pathogenic variants in *DNAH5* also demonstrated a negative correlation with neonatal complications requiring intensive care, while exhibiting comparative attenuation in clinical severity and preserved pulmonary function [18].

Rare variants in *DNAH6* (n = 2), a gene encoding a novel dynein motor protein [19], demonstrate critical roles in left-right patterning and ciliary function, with its mutations strongly implicated in the pathogenesis of heterotaxy. Li et al. demonstrated that *DNAH6* contributes to heterotaxy and PCD via both recessive mutations and trans-heterozygous interactions with other PCD genes (e.g. *DNAH5*, *DNAI1*), using morpholino knockdown in zebrafish or shRNA-mediated silencing in human/mouse respiratory epithelia [20]. This digenic interaction of *DNAH6* with *DNAH5* aligns with the phenotypic characteristic and outcome observed in case 6 of our cohort, as detailed in Table 2. Their findings propose an oligogenic model for ciliopathies, broadening the understanding of genetic complexity in left-right patterning disorders.

MYO1D (myosin 1D), an unconventional myosin isoform, has been implicated as the first actin-dependent molecular motor regulating left-right (LR) axis specification in Drosophila [21, 22], zebrafish [23, 24], and *Xenopus laevis* [25, 26]. Despite its conserved role in model organisms, *MYO1D* has not yet been established as a pathogenic determinant of human laterality disorders, with no validated mutations reported in clinical cohorts to date. The c.2293C > T (p. Pro765Ser) missense variant in *MYO1D* was initially identified in a 4.5-year-old proband of Arab descent presenting with HTX and complex congenital heart disease, born to consanguineous parents. While in silico predictive analyses provided supporting evidence for pathogenicity, validation through functional studies remains lacking. Collectively, these findings propose *MYO1D* as a candidate gene for HTX under an AR inheritance model within this familial context [27]. Yuan et al. identified biallelic *MYO1D* variant (c.1531G > A: p.D511N) as novel genetic determinants of laterality defects, congenital heart disease, and sperm defects in humans. Together with the above reported *MYO1D* variant (c.2293C > T: p. Pro765Ser), integrative approach combining WES, structural modeling, and functional assays were applied to confirm *MYO1D*'s dual role in developmental asymmetry and reproductive health [28]. In our prenatal cohort, two variants in *MYO1D* were detected in case 3, including one missense variant (c.2419G > A: p.V807M) and one intronic variant (c.619-182G > A), together with three variants in *DNAH11* gene (OMIM: 611884) and two variants in *DNAH9* gene (OMIM: 618300). The specific genetic mode and precise molecular mechanism remain to be fully elucidated.

*RFX3* gene, identified in case 17, encoding a transcription factor (Regulatory Factor X3) involved in the control of ciliogenesis [29]. By generating Rfx3-deficient mice, Bonnafe et al. demonstrated that RFX3 governs nodal cilium development by regulating *D2lic* gene, a retrograde intraflagellar transport component, thereby essential for vertebrate LR axis specification [30]. Robson et al. demonstrated that histone H2B monoubiquitination (H2Bub1) regulates cardiac left-right patterning by epigenetically controlling Rfx3-dependent cilia motility, linking chromatin remodeling defects to congenital heart disease through impaired transcriptional activation of ciliary genes [31]. However, to date, *RFX3* gene variants have not been conclusively demonstrated to exhibit a direct association with the pathogenesis of HTX in humans.

Our findings were in concordance with previous studies. Recent study in targeted sequencing demonstrated higher coverage and superior cost-efficacy for monogenic obesity and diabetes mellitus diagnosis compared to WES, with a similar diagnostic yield ( 32.9% vs. 32.2% ) at reduced cost (~ 5 pounds/sample vs. >100 pounds/sample) [32]. A prospective cohort study demonstrated that multidisciplinary-guided prenatal exome trio sequencing achieved 81% diagnostic accuracy (13/16 cases) for skeletal dysplasias, enabling precise prenatal counseling through virtual gene panel analysis (240 skeletal dysplasias genes) [33].

## Limitations

While this study provides novel insights into the genetic architecture of human laterality defects, several limitations should be acknowledged. The relatively small sample size restricts the statistical power to detect rare variants or subtle genotype-phenotype correlations. The lack of familial samples for segregation analysis precludes definitive confirmation of inheritance patterns (e.g. de novo vs. inherited) and assessment of variant penetrance. The absence of in vitro or in vivo functional validation limits mechanistic understanding of identified variants.

## Conclusion

In conclusion, this work advances prenatal diagnostics by delineating specific advantages integrating technical comparisons, cost-benefit analyses, and novel biological insights of customized targeted gene panel and WES approaches, introduces a cross-species framework for gene prioritization, and delivers actionable protocols to enhance diagnostic efficiency. Accurate prenatal diagnosis of fetal laterality defects serves as a cornerstone for risk stratification,

parental counseling, and tailored obstetric-neonatal care pathways. By integrating advanced imaging, genetic testing, and multidisciplinary collaboration, clinicians can mitigate neonatal morbidity and empower families through evidence-based decision-making. Our findings underscore the critical role of epigenomic-ciliary interplay in heterotaxy pathogenesis, with broad implications for congenital anomaly management.

## Declarations

**Ethics approval and consent to participate**

This study was approved by the Institutional Review Board (IRB) of the Women's Hospital, Zhejiang University, School of Medicine (Approval No. IRB-20240066-R) and was conducted in full compliance with the Declaration of Helsinki. Written informed consent was obtained from all enrolled participants.

**Consent for publication**

Not applicable.

**Availability of data and materials**

The raw sequence data reported in this paper have been deposited in GSA-Human (HRA018279) that are publicly accessible at https://ngdc.cncb.ac.cn/gsa-human.

**Competing interests**

The authors declare no competing interests.

**Funding**

This work was supported by grants from 4+X Clinical Research Project of Women's Hospital, School of Medicine, Zhejiang University (ZDFY2023-4X202).

**Authors contributions**

Conceptualization YC, PFX; data curation YC, YQQ; formal analysis YC, YQQ; funding acquisition YC; methodology YQQ, PFX; writing original draft YC, YQQ; writing review and editing PFX, QL.

**Acknowledgements**

We are grateful to all the patients and families who contributed their data to this research. The authors also acknowledge the technical assistance and next-generation sequencing services provided by Hangzhou Yizhen Medical Laboratory, China and BGI Medical Laboratory, Shenzhen, China.

**Authors information**

Not applicable.

## References

1. Soof M, Alpert MA, Barbadora J, Mukerji B, Mukerji V. Human laterality disorders: pathogenesis, clinical manifestations, diagnosis, and management. Am J Med Sci. 2021;362:233–42.
2. Eitler K, Bibok A, Telkes G. Situs Inversus Totalis: A Clinical Review. Int J Gen Med. 2022;15:2437–49.
3. Grimes DT, Burdine RD. Left-right patterning: breaking symmetry to asymmetric morphogenesis. Trends Genet. 2017;33(9):616–28.
4. Shapiro AJ, Davis SD, Ferkol T, Dell SD, Rosenfeld M, Olivier KN, et al. Genetic Disorders of Mucociliary Clearance Consortium. Laterality defects other than situs inversus totalis in primary ciliary dyskinesia: insights into situs ambiguus and heterotaxy. Chest. 2014;146(5):1176–86.
5. Kahraman FU, Jafarov U, Yazan H, Yurtsever I, Cakir E, Sayin GY. Evaluation of the Clinical and Genetic Characteristics of Primary Ciliary Dyskinesia Patients With Situs Inversus Totalis. Birth Defects Res. 2025;117(2):e2444. 10.1002/bdr2.2444.
6. Kuehl KS, Loffredo C. Risk factors for heart disease associated with abnormal sidedness. Teratology. 2002;66:242–8.
7. Li AH, Hanchard NA, Azamian M, D'Alessandro LCA, Coban-Akdemir Z, Lopez KN, et al. Genetic architecture of laterality defects revealed by whole exome sequencing. Eur J Hum Genet. 2019;27(4):563–73.
8. Buca DIP, Khalil A, Rizzo G, et al. Outcome of prenatally diagnosed fetal heterotaxy: systematic review and meta-analysis. Ultrasound Obstet Gynecol. 2018;51:323–30.
9. Belmont JW, Mohapatra B, Towbin JA, et al. Molecular genetics of heterotaxy syndromes. Curr Opin Cardiol. 2004;19:216–20.
10. Lee IH, Lin Y, Alvarez WJ, Hernandez-Ferrer C, Mandl KD, Kong SW. WEScover: selection between clinical whole exome sequencing and gene panel testing. BMC Bioinformatics. 2021;22(1):259.
11. Li H, Durbin R. Fast and accurate short read alignment with Burrows-Wheeler transform. Bioinformatics. 2009;25(14):1754–60.
12. McKenna A, Hanna M, Banks E, Sivachenko A, Cibulskis K, Kernytsky A, et al. The Genome Analysis Toolkit: a MapReduce framework for analyzing next-generation DNA sequencing data. Genome Res. 2010;20(9):1297–303.

13. Richards S, Aziz N, Bale S, Bick D, Das S, Gastier-Foster J, et al. Standards and guidelines for the interpretation of sequence variants: a joint consensus recommendation of the American College of Medical Genetics and Genomics and the Association for Molecular Pathology. Genet Med. 2015;17:405–24.
14. Okonechnikov K, Conesa A, García-Alcalde F. Qualimap 2: advanced multi-sample quality control for high-throughput sequencing data. Bioinformatics. 2016;32(2):292–4.
15. Monaghan KG, Leach NT, Pekarek D, Prasad P, Rose NC, ACMG Professional Practice and Guidelines Committee. The use of fetal exome sequencing in prenatal diagnosis: a points to consider document of the American College of Medical Genetics and Genomics (ACMG). Genet Med. 2020;22(4):675–80.
16. Hornef N, Olbrich H, Horvath J, Zariwala MA, Fliegauf M, Loges NT, et al. DNAH5 mutations are a common cause of primary ciliary dyskinesia with outer dynein arm defects. Am J Respir Crit Care Med. 2006;174(2):120–6.
17. Emiralioğlu N, Taşkıran EZ, Koşukcu C, Bilgiç E, Atilla P, Kaya B, et al. Genotype and phenotype evaluation of patients with primary ciliary dyskinesia: First results from Turkey. Pediatr Pulmonol. 2020;55(2):383–93.
18. Davis SD, Ferkol TW, Rosenfeld M, Lee HS, Dell SD, Sagel SD, et al. Clinical features of childhood primary ciliary dyskinesia by genotype and ultrastructural phenotype. Am J Respir Crit Care Med. 2015;191(3):316–24.
19. Hom EF, Witman GB, Harris EH, Dutcher SK, Kamiya R, Mitchell DR, et al. A unified taxonomy for ciliary dyneins. Cytoskeleton (Hoboken). 2011;68(10):555–65.
20. Li Y, Yagi H, Onuoha EO, Damerla RR, Francis R, Furutani Y, et al. DNAH6 and Its Interactions with PCD Genes in Heterotaxy and Primary Ciliary Dyskinesia. PLoS Genet. 2016;12(2):e1005821.
21. Hozumi S, Maeda R, Taniguchi K, Kanai M, Shirakabe S, Sasamura T, et al. An unconventional myosin in Drosophila reverses the default handedness in visceral organs. Nature. 2006;440:798–802.
22. Spéder P, Adám G, Noselli S. Type ID unconventional myosin controls left-right asymmetry in Drosophila. Nature. 2006;440:803–7.
23. Juan T, Geminard C, Coutelis JB, Cerezo D, Polès S, Noselli S, et al. Myosin1D is an evolutionarily conserved regulator of animal left-right asymmetry. Nat Commun. 2018;9:1942.
24. Lebreton G, Geminard C, Lapraz F, Pyrpassopoulos S, Cerezo D, Spéder P, et al. Molecular to organismal chirality is induced by the conserved myosin 1D. Science. 2018;362:949–52.
25. Tingler M, Kurz S, Maerker M, Ott T, Fuhl F, Schweickert A et al. A conserved role of the unconventional myosin 1D in laterality determination. Curr Biol. 2018;28:810 – 16.e813.
26. Yuan S, Brueckner M. Left-right asymmetry: myosin 1D at the center. Curr Biol. 2018;28:R567–9.
27. Alsafwani RS, Nasser KK, Shinawi T, Banaganapalli B, ElSokary HA, Zaher ZF, et al. Novel MYO1D Missense Variant Identified Through Whole Exome Sequencing and Computational Biology Analysis Expands the Spectrum of Causal Genes of Laterality Defects. Front Med (Lausanne). 2021;8:724826.
28. Yuan Z, Zhu X, Xie X, Wang C, Gu H, Yang J, et al. Identification of a novel MYO1D variant associated with laterality defects, congenital heart diseases, and sperm defects in humans. Front Med. 2024;18(3):558–64.
29. Thomas J, Morlé L, Soulavie F, Laurençon A, Sagnol S, Durand B. Transcriptional control of genes involved in ciliogenesis: a first step in making cilia. Biol Cell. 2010;102(9):499–513.
30. Bonnafe E, Touka M, AitLounis A, Baas D, Barras E, Ucla C, et al. The transcription factor RFX3 directs nodal cilium development and left-right asymmetry specification. Mol Cell Biol. 2004;24(10):4417–27.
31. Robson A, Makova SZ, Barish S, Zaidi S, Mehta S, Drozd J, et al. Histone H2B monoubiquitination regulates heart development via epigenetic control of cilia motility. Proc Natl Acad Sci U S A. 2019;116(28):14049–54.
32. Yu H, Yu H, Zhang R, Peng D, Yan D, Gu Y, et al. Targeted gene panel provides advantages over whole-exome sequencing for diagnosing obesity and diabetes mellitus. J Mol Cell Biol. 2023;15(6):mjad040.
33. Chandler N, Best S, Hayward J, Faravelli F, Mansour S, Kivuva E, et al. Rapid prenatal diagnosis using targeted exome sequencing: a cohort study to assess feasibility and potential impact on prenatal counseling and pregnancy management. Genet Med. 2018;20(11):1430–7.

## Figures

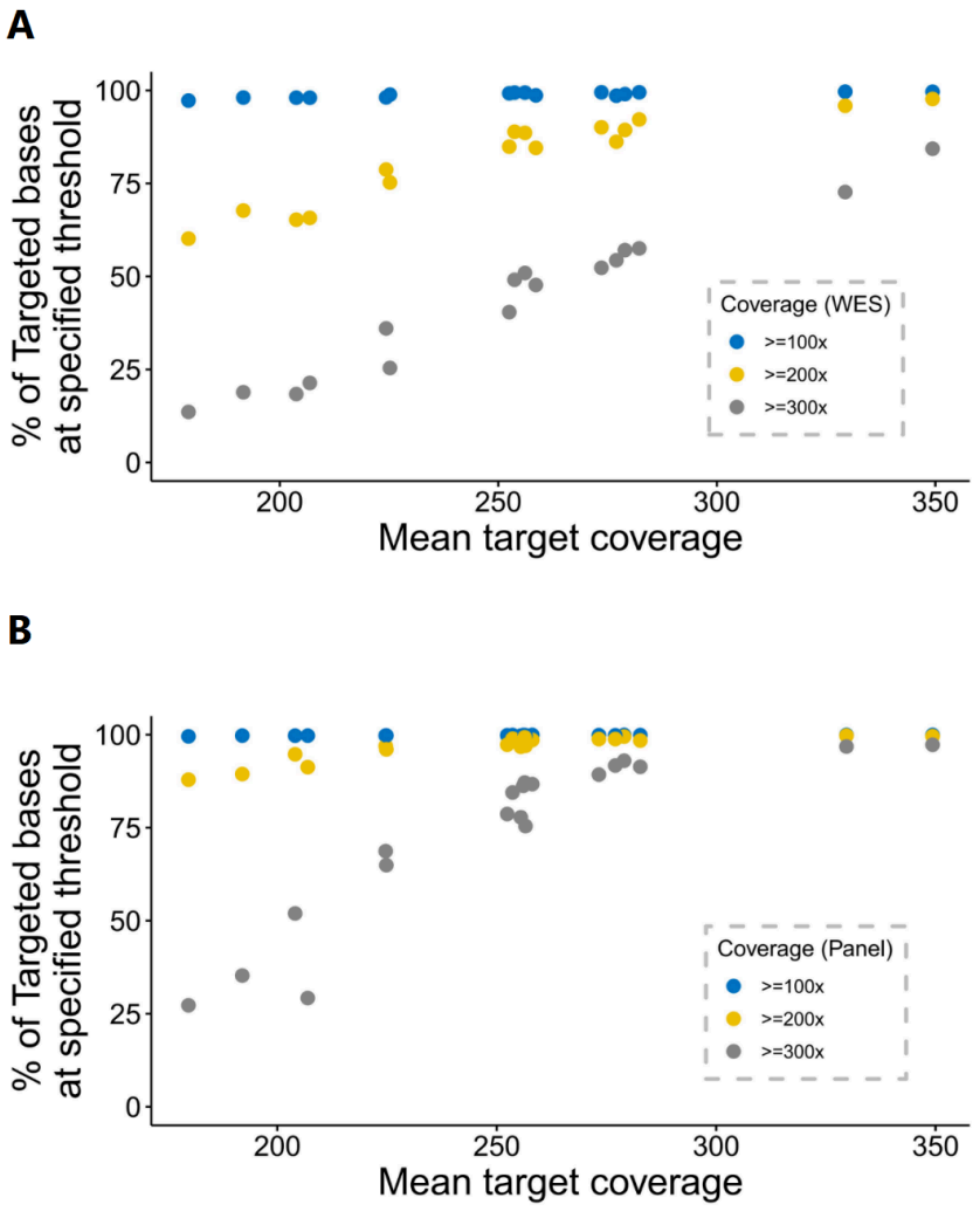



**Figure 1**

**Coverage of samples assayed by WES and Panel.**

The scatter plots show the percentage of targeted bases that exceeded specified coverage thresholds in the WES (A) and Panel (B) samples, respectively. The Panel samples were down-sampled to align with the average read counts of the corresponding WES samples, enabling comparison at the same sequencing read depth. Each sample is represented by a set of three dots, color-coded to indicate different coverage thresholds. The x-axis displays the mean target coverage for each sample, while the y-axis shows the percentage of reads with coverage above the specified threshold.

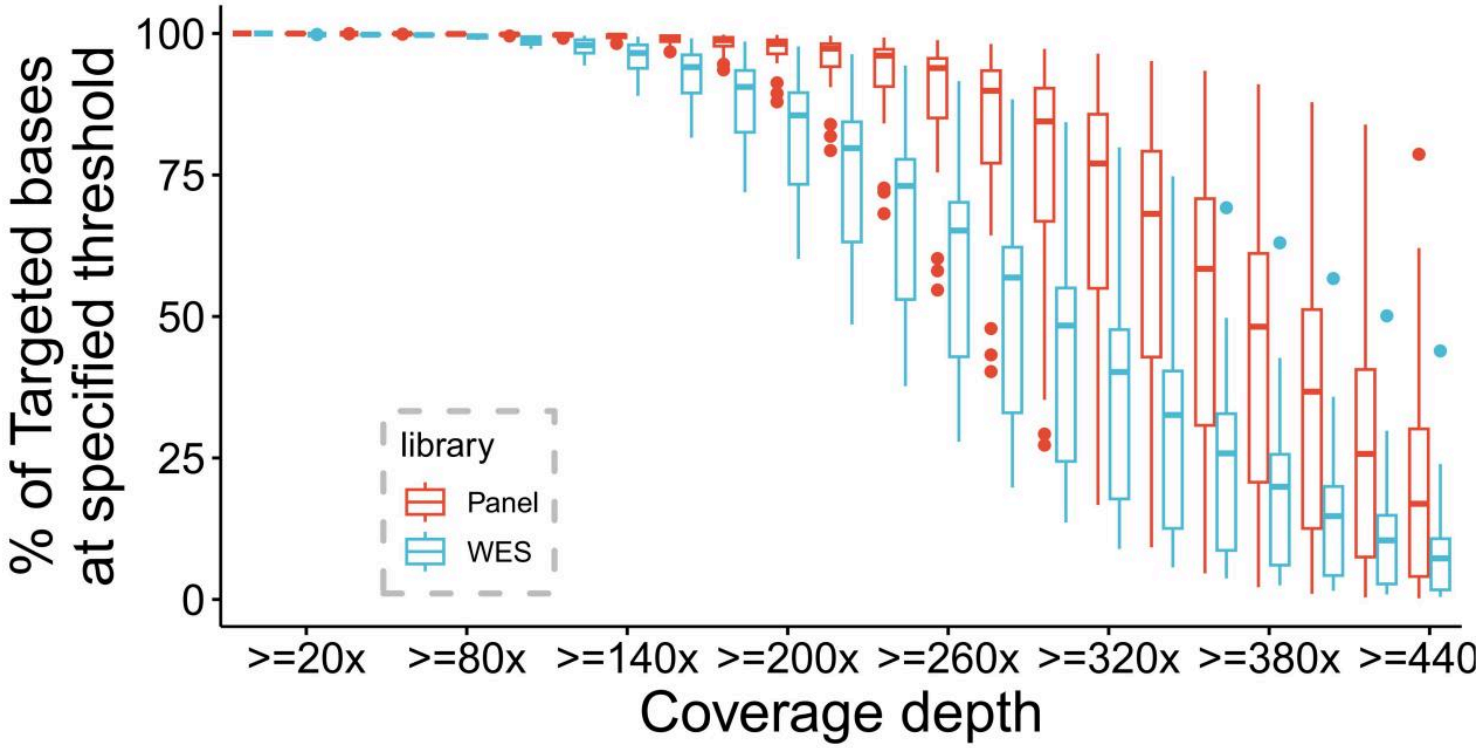



**Figure 2**

**Distribution of coverage across multiple depth thresholds for WES and Panel samples.**

The x-axis represents different coverage depth thresholds. The y-axis shows the percentage of targeted bases that meet or exceed each coverage depth threshold. The central line in each box denotes the median percentage coverage, the edges of the box are the interquartile range (IQR), and the whiskers extend to the furthest data point within 1.5 times the IQR from the box.